

# Orientation of the alkyl side chains and glucopyranose rings in Langmuir–Blodgett films of a regioselectively substituted cellulose ether

Wakako Kasai · Keisuke Tsutsumi · Mitsuhiro Morita · Tetsuo Kondo

Received: 29 March 2007 / Revised: 22 November 2007 / Accepted: 1 December 2007 / Published online: 19 December 2007  
© Springer-Verlag 2007

**Abstract** An arrangement for the long alkyl side chains in a Langmuir–Blodgett (LB) film from regioselectively alkylated 2,3-di-*O*-octadecylcellulose on an Au-coated substrate was investigated using Fourier transform infrared reflection absorbance spectroscopy. The IR results indicated that the hydrophobic long alkyl side chains were forced to be repellent to the surface of water, resulting in deposition on the substrate, with it being tilted in the vertical direction, and further formed both hexagonal and orthorhombic crystalline structures up to 10 layers in the LB film. In addition, molecular modeling with CAChe software indicated that the optimized assembly of the side chains was supposed to own a vertical arrangement against the substrate surface after compression of the monolayer. This means that the conformation of  $2_1$  screw of the cellulose molecular chain may be altered by the compression to have an unusual conformation by a different  $\phi$ – $\psi$  dihedral angle such as onefold axis without a symmetry element.

**Keywords** Cellulose · Langmuir–Blodgett film · FTIR-RAS · Orientation

## Introduction

Langmuir–Blodgett (LB) films are prepared by the successive deposition of monolayers from the air–water interface onto a solid substrate. By using the LB technique, functional films can be fabricated with desired properties. Thus, the films have possibility as the microelectronics and biomimetic membranes by incorporating functional groups having various effects, such as optics, electroconductivity, and magnetics. To extend the function of such LB membranes, it is of importance to characterize the assembly state of the composed molecules. Side chain orientation in LB films has been extensively investigated by Fourier transform infrared reflection absorbance spectroscopy (FTIR-RAS) [1, 2]. The technique monitors molecular vibrations that produce dipole moment oscillations. The observed frequencies are dependent on molecular conformation and configuration. In particular, p-polarized FTIR-RAS can provide useful information on the conformational state of the hydrocarbon chain in the monolayer on the substrate [1, 2]. Almost all LB films composed of low-molecular-weight molecules, such as fatty acid films, are unstable with regard to heating, mechanical treatment, and high vacuum [3, 4]. On the contrary, some polymers were found to form stable LB films [5, 6]. It was also found that cellulose derivatives having alkyl side chains formed stable LB films [7–9].

Cellulose is the most abundant natural resource on the earth, and this biomacromolecule is, of course, biodegradable. However, the usage of cellulose at present is limited mainly to structural materials such as pulp and wood-based materials. Because cellulose forms a crystalline structure during the biosynthesis, it is stable against heat, light, and chemicals except strong acids, thereby causing insolubility

W. Kasai · T. Kondo (✉)  
Bio-Architecture Center (KBAC), Kyushu University,  
6-10-1, Hakozaki,  
Fukuoka 812-8581, Japan  
e-mail: tekondo@agr.kyushu-u.ac.jp

K. Tsutsumi · M. Morita · T. Kondo  
Graduate School of Bioresource and Bioenvironmental Sciences,  
Kyushu University,  
6-10-1, Hakozaki,  
Fukuoka 812-8581, Japan

in usual single solvents to result in the limited usage. Thus, it is required for native cellulose materials to be modified in a facile and low-energy cost fashion to add versatility of functions. To develop a new direction of cellulose usage as advanced functional materials, the LB technique is one of the promising methods to obtain desired structures and properties at the nanoscale.

In our previous report [9], regioselectively substituted *O*-alkylcellulose ethers having long alkyl side chains, 6-*O*-(6C18), 2,3-di-*O*-(23C18), and tri-*O*-octadecyl-celluloses (triC18), were synthesized, and they were transferred on a mica substrate to yield the LB monolayers. Then, the 23C18 LB monolayer only exhibited homogeneous at the nanoscale when compared with other samples judging from AFM and X-ray results. The structure of the cellulosic monolayers might be affected by distribution of the alkyl side chains and lack of inter- and/or intramolecular hydrogen bonds engaged in the molecules. Concerning orientation in general appeared in LB films of cellulose derivatives, there are four aspects that should be considered: (1) side chain orientation, (2) glucopyranose ring arrangements, (3)  $2_1$  screw axis with respect to glucopyranose ring arrangements, and (4) molecular chain orientation. In this LB monolayer of regioselectively substituted 23C18, it was suggested that the glucopyranose ring planes were arranged in a direction perpendicular to the substrate. The results indicated that distribution of the substituent played a more important role in the molecular assembly rather than degree of substitution (DS). However, to date, the correlation between regioselectivity of side chains and the monolayer structure has been rarely investigated, although the preparation and characterization of monolayers and LB films of cellulose derivatives having different DS has been extensively examined [10, 11].

Recently, we developed a unique form  $\beta$ -glucan association, “nematic ordered cellulose (NOC)” [12]. NOC is prepared by uniaxial stretching of water-swollen cellulose from the *N,N*-dimethylacetamide (DMAc)/LiCl solution, and thereby, the cellulose molecular chains tend to be oriented toward the stretching axis [13]. Further, the hydroxymethyl (OH) groups at the C-6 position that are equatorial-bonded to the anhydroglucose unit are stuck up against the surface and tilted from the perpendicular. Between the hydrophilic molecular tracks due to OH groups, the hydrophobic phase due to the anhydroglucose plane also appeared, resulting in both hydrophilic and hydrophobic tracks next to each other across the NOC surface. These amphiphilic molecular tracks enhance the unique surface properties of NOC [14]. It is indicated that properties of cellulosic materials are strongly affected by the molecular assemble state. Therefore, the study of the correlation between the molecular assembly depending on regioselectivity of side chains and the monolayer structure is very important.

In this article, we have first attempted to characterize, using IR-RAS, the orientation of the long alkyl side chains in a LB film of regioselectively substituted cellulose ether “23C18,” which could provide a homogeneous film at the nanoscale [9]. Furthermore, a molecular modeling method based on the above results has been applied to examine the glucopyranose ring arrangement with respect to the  $2_1$  screw axis of the cellulose molecular chain.

## Experimental

### Sample for LB films

2,3-Di-*O*-octadecylcellulose (23C18) was prepared from 6-*O*-triphenylmethylcellulose (tritylcellulose) with a DP of 180 as the starting material by a modified procedure of Kondo and Gray [15]. IR and NMR analyses identified that the synthesized compound was indeed 2,3-di-*O*-octadecylcellulose, as shown in Fig. 1 [9]. Significant depolymerization did not occur during the alkylation process, based on the result of size-exclusion chromatograms [9, 15]. Therefore, DP of the cellulose samples thus prepared should have almost the same value (DP=180) of the starting material. Details of the synthesis and characterization are given in our previous paper [9].

### Preparation of LB film of 23C18

The cellulose ether was dissolved in dichloromethane to provide a clear solution of 10 – 15  $\mu$ l at a concentration of 0.05% (w/v). The solution was spread on a clean water surface in a Teflon-coated trough (40 $\times$ 200 mm<sup>2</sup>). The water as a subphase was purified by NANOpure Diamond Ultrapure Water Systems (Barnstead International, Dubuque, IA, USA). The monolayer compression with Teflon-coated barrier was started 30 min after the addition of the solution on the water, allowing the solvent to completely evaporate from the water surface. The compression rate was 8 mm/min and the surface pressure was recorded by the Wilhelmy method [16]. The compression isotherm of 23C18 is shown in Fig. 2 [9]. The monolayer was transferred to an Au-coated microscopic slide by the vertical dipping method at the surface pressure of 7.5 mN/m. Deposition speeds of 8 and

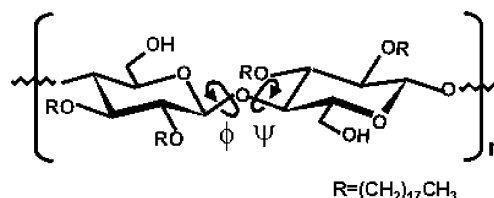


Fig. 1 Chemical structure of 2,3-di-*O*-octadecyl-cellulose (23C18)

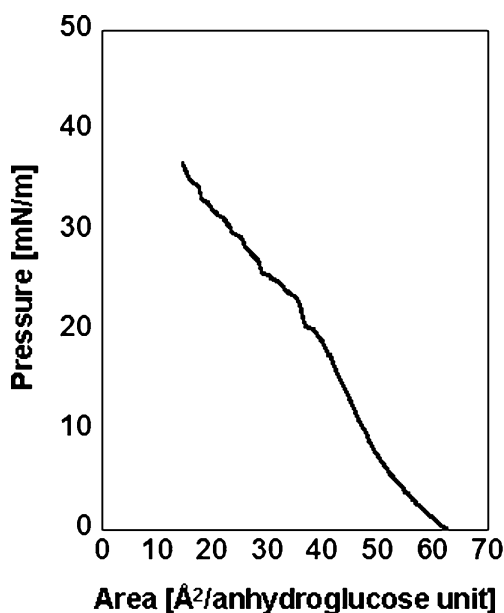


Fig. 2 The compression isotherm of 23C18

60 mm/min were employed for the up and down strokes, respectively. Then, LB films with odd and even numbers of accumulated monolayers were transferred to the substrate using down and up strokes, respectively.

The transfer ratio of the first layered LB films was 0.5, whereas those of 2-, 4-, 6-, and 10-layered LB films were  $1.0 \pm 0.2$ . Although it was difficult to transfer the first layer of LB film onto the Au-coated microscopic slide, the 2nd–10th layers of LB film were successfully transferred to the substrate.

## Measurements

Fourier transform infrared reflection absorbance spectroscopy (FTIR-RAS)

Infrared spectra were recorded with a JASCO FT/IR-620 equipped with a RAS-400 attachment with a polarizer using a MCT detector. For the measurements of infrared

reflection absorbance (RA) spectra, a reflection accessory was employed at the incident angle of  $80^\circ$  together with a KRS-5 (thallium bromide–iodide) polarizer. Sixty-four scans were averaged with a resolution of  $2 \text{ cm}^{-1}$ . The wavenumber region investigated ranged from  $4,000$  to  $900 \text{ cm}^{-1}$ . The monolayers deposited on the Au-coated microscopic slides mentioned above were provided for the IR-RAS measurements.

## Molecular modeling

Molecular modeling was performed by CAChe (Fujitsu, Tokyo, Japan). The molecular structure was optimized by MM2 and PM3 methods. The processes for this molecular modeling are described in the “[Result and Discussion](#)” section.

## Results and discussion

Characterization of the alkyl side chain orientation using FTIR-RAS

Figure 3a and b show a RA spectrum of the two layers of accumulated LB film and a transmission spectrum of the cast film of 2,3-di-*O*-octadecylcellulose (23C18) in the CH stretching region ( $2,800$ – $3,000 \text{ cm}^{-1}$ ), respectively. The information on molecular orientation can be given by comparison between RA spectrum and transmission spectrum. Using RAS, information of the IR spectrum with E parallel to the incidence plane on a metal surface is obtained. Therefore, if the alkyl side chains stuck to the surface in the LB films, five absorption bands ( $2,962$ ,  $2,927$ ,  $2,918$ ,  $2,873$ , and  $2,850 \text{ cm}^{-1}$ ) due to vibrations of the alkyl side chains are detected in the RA spectrum [17]. The five bands could be identified in the following: The  $\text{CH}_3$  stretching bands, found at  $2,962$ ,  $2,927$ , and  $2,873 \text{ cm}^{-1}$ , were assigned to asymmetric [ $\nu_a(\text{CH}_3)$ ] in skeletal plane and two symmetric [ $\nu_s(\text{CH}_3)$ ]  $\text{CH}_3$  stretching vibrations, respectively. The  $\text{CH}_2$  stretching bands, found at

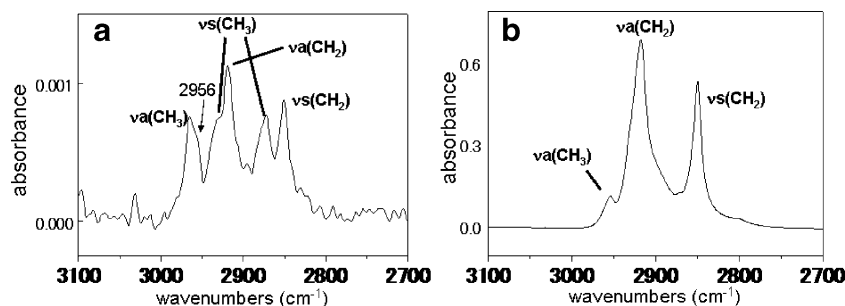
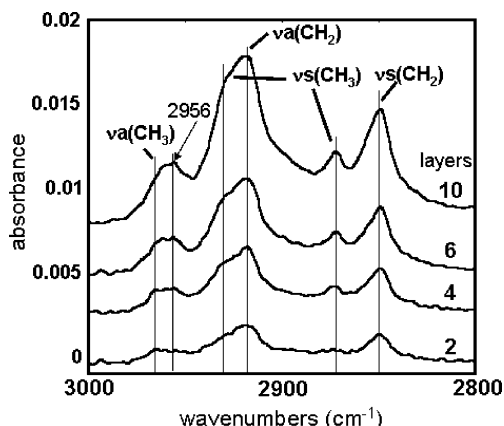


Fig. 3 Infrared spectra of 23C18 in the CH stretching region; a a RA spectrum of two layers of accumulated LB film of 23C18 on an Au-coated microscopic slide and b a transmission spectrum of the 23C18 cast film

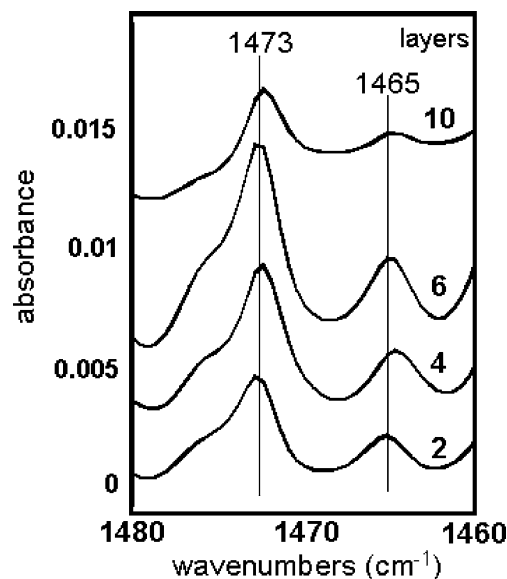
2,918 and 2,850  $\text{cm}^{-1}$ , were assigned to asymmetric [ $\nu_a(\text{CH}_2)$ ] and symmetric [ $\nu_s(\text{CH}_2)$ ]  $\text{CH}_2$  stretching vibrations, respectively. As shown in Fig. 3a, five absorption bands (2,962, 2,927, 2,918, 2,873, and 2,850  $\text{cm}^{-1}$ ) were actually observed in the RA spectrum. However, if a long alkyl chain is perfectly perpendicular to the surface, the band assigned to the [ $\nu_a(\text{CH}_3)$ ] at 2,956  $\text{cm}^{-1}$  due to the out-of-skeletal plane shown by the arrow in Fig. 3a should not be observed in RAS measurements [18]. It indicated that the long alkyl side chains were slightly tilted. Moreover, the appearance of the bands at 2,918 and 2,850  $\text{cm}^{-1}$  due to [ $\nu_a(\text{CH}_2)$ ] and [ $\nu_s(\text{CH}_2)$ ], respectively, may correspond to the previous report that the alkyl chains were in the all-trans conformation in the hexagonal lattice [19]. On the contrary, as 23C18 in the cast film (Fig. 3b) had a random orientation with respect to the substrate surface, the  $\text{CH}_2$  and  $\text{CH}_3$  groups were supposedly present without a particular order. Therefore, intensity of  $\text{CH}_2$  stretching vibrations with large amounts in the 23C18 was naturally strong when compared with that of  $\text{CH}_3$  stretching vibrations at 2,927 and 2,873  $\text{cm}^{-1}$  located at the end of the side chain in the cast film, as shown in Fig. 3b.

Figure 4 shows RA spectra of 2, 4, 6, and 10 layers of accumulated LB films of 23C18 in the CH stretching region. The five bands and [ $\nu_a(\text{CH}_3)$ ] bands at 2,956  $\text{cm}^{-1}$  as, are shown in Fig. 3a, were also observed at all the films in Fig. 4. In addition, Fig. 4 shows that the more layers are accumulated, the stronger and sharper the absorption bands become. This indicates that the alkyl side chain ordering could be maintained up to 10 layers, and the side chains were packed in the LB film without deformation, though the alkyl side chains were tilted slightly from the perpendicular direction as already described.

Figure 5 shows RA spectra of 2, 4, 6, and 10 layers of accumulated LB films of 23C18 in the  $\text{CH}_2$  scissoring region. The intensity of the IR spectrum for the 10 layers' accumulated LB film is smaller when compared with those



**Fig. 4** Infrared RA spectra of 2, 4, 6, and 10 layers of accumulated LB films of 23C18 in the CH stretching region



**Fig. 5** Infrared RA spectra of 2-, 4-, 6- and 10 layers' accumulated LB films of 23C18 in the  $\text{CH}_2$  scissoring region

for 2, 4, and 6 layers of accumulated LB films. This indicates that the structure of the 10 layers of accumulated LB film might be partially destroyed, although some of the side chain orientation still remained. The two bands observed at 1,473 and 1,465  $\text{cm}^{-1}$  in all the films of Fig. 5 were assigned to  $\text{CH}_2$  bending [ $\delta(\text{CH}_2)$ ] vibrations. These bands are so-called typical “crystalline bands,” which are characteristics of *n*-paraffins crystallized with an orthorhombic subcell packing of  $\text{CH}_2$  groups [17, 20]. However, as these IR absorption bands, when the molecular chain axis is perfectly parallel to *p*-polarized beam, should not be usually observed in the RAS measurements [17], the long alkyl side chains exhibiting such IR bands also proved to be slightly tilted, as mentioned above. Moreover, as described already, we had evidence that the alkyl chains were in all-trans conformation in the hexagonal lattice. It indicated that there are two crystal structures due to alkyl side chains in LB film. *n*-Octadecanol in the monolayers form various polymorphism such as orthorhombic and hexagonal structures depending on the surface pressure and temperature [21–25]. In this preparation of LB film, as monolayer was compressed by a barrier, phase transition of crystal structure from alkyl side chains might be caused by the pressure. Although the resolution of the IR measurement in the present case was not sufficiently well to be discussed on the conformation, the presence of a mixture of orthorhombic and hexagonal structures was indicated.

#### Molecular modeling by CAChe

What would be the stable conformation of the 23C18 on the water surface? In general, a cellulose molecular chain owns the  $2_1$  screw axis. Figure 6a shows that the structure of

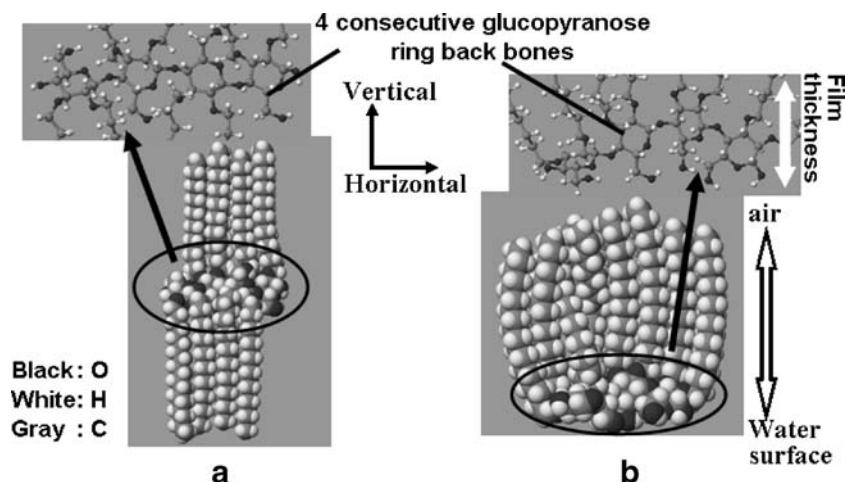


**Fig. 6** Molecular model of 23C18 based on four consecutive glucopyranose rings by CAChe (MM2 and PM3); **a** a usual stabilized state and **b** a LB monolayered state. The space-filling models indicate

23C18, whereas the cylinder ball models indicate the glucose backbone of the 23C18 in each state

23C18 was optimized by CAChe (MM2 and PM3 methods) based on the conformation of  $2_1$  screw of the cellulose backbone. First, the structure of cellotetraose was optimized by a PM3 method. Continuously, 23C18 was optimized by a MM2 method after OH groups at the C2 and C3 positions of anhydroglucose unit were replaced by the C18 alkyl groups. As a result, the procedure provided the stabilized structure of 23C18 as shown in Fig. 6a. Next, the 23C18 structure in LB monolayer was optimized by CAChe (MM2 and PM3 methods) based on FTIR-RAS results in this study. From the results of the IR measurements, C18 alkyl side chains of 23C18 monolayer were stuck to the substrate surface. Therefore, as a first step, C18 alkyl side chains were aligned perpendicular against the substrate surface. Glucose planes of cellotetraose were aligned parallel to the surface. Then, C18 alkyl side chains and glucose units were combined and optimized by MM2 and PM3 methods, resulting in the stabilized structure of LB monolayer, as shown in Fig. 6b. This indicates that the conformation of  $2_1$  screw of the cellulose backbone (as indicated in Fig. 1) may be altered to have an unusual  $\phi$ - $\psi$  dihedral angle corresponding to a onefold axis without a symmetry element in the monolayer during the compression.

Native cellulose crystals (cellulose I) are supposed to have two different intramolecular hydrogen bonds, which are between the OH at the C3 position (OH-3) and adjacent ring O-5 and between the OH at the C6 position (OH-6) and adjacent OH at the C2 position (OH-2) of the neighboring ring. The presence of these hydrogen bonds is indirectly connected with the stability of the conformation of  $2_1$  screw of the cellulose. Because OH-2 and -3 were selectively blocked, in the case of 23C18 cellulose, the intramolecular hydrogen bonds between the OH-3 and adjacent ring O-5 are inhibited to form. Therefore,

conformation of 23C18 cellulose backbone in the LB monolayer may be rearranged into the onefold axis during the compression because conformation of 23C18 cellulose backbone is not stabilized when compared with that of native cellulose crystals. Moreover, it is suggested that the long alkyl side chains at the C2 and C3 positions stood up against the water surface to be crystallized, whereas OH groups at the C6 position may be facing the water surface during compression of the monolayer. Finally, the optimized situation of anhydroglucose rings of the 23C18 LB film was obtained to be in a vertical arrangement against the substrate, as shown in Fig. 6b. This molecular conformation with consideration of hydrogen bonding in the compound also supported the result of our previous report on this 23C18 LB monolayer [9].

## Conclusion

Orientation of the long alkyl side chain of the 23C18 LB film on the Au-coated microscopic slide was investigated using FTIR-RAS. The analyses revealed that the long alkyl side chains axis stood against the substrate though the side chains were slightly tilted. It also indicated that the hexagonal and orthorhombic crystalline structures might be formed among the side chains up to 10 layers of the LB film. It was reported that octadecanol undergoes several phase transitions depending on the pressure and temperature by X-ray diffraction [24, 25]. In the case of layers transferred to a solid substrate, the coexistence of hexagonal and orthorhombic structures could rather be a reflection of the coexistence of nontilted and tilted chains. As in many other cases, the transfer can induce changes in the molecular orientation and packing of the molecules due to



a different interaction with the underlying layers. Here, this IR investigation cannot provide information of the compressed structure for 23C18 LB film on the water surface because only the structure of 23C18 LB film on the substrate was focused on in this study. The assembled monolayer structure of the LB film was also investigated by a molecular modeling method using CAChe. The optimized situation of the glucopyranose ring of the 23C18 LB film was obtained to be in a vertical arrangement against the substrate. Then, it should be noted that conformation of  $2_1$  screw of the cellulose backbone was assumed to be altered to have an unusual  $\phi$ – $\psi$  dihedral angle corresponding to a onefold axis without a symmetry element in the monolayer during the compression. As IR-RAS indicated, the side chain arrangement to provide the crystallization may facilitate compensating and stabilizing the free energy of the unusual conformation in the cellulose molecules, as shown in Fig. 6b. It is also suggested that the homogeneous and smooth surface of the 23C18 LB film as previously reported may be caused by the alkyl side chains crystals [9]. These suggestions lead to the fact that distribution of the long alkyl substituents had a strong correlation with the orientation of arrangements in both the side chains and the glucopyranose ring in the regioselectively substituted *O*-alkylcellulose when it was transferred into the LB films. The molecular chain orientation is the subject of our further investigation, aimed at the fabrication of advanced functionalized materials from cellulose.

**Acknowledgements** This research was supported partly by a Grant-in-Aid for Scientific Research (No. 14360101), Japan Society for the Promotion of Science (JSPS). The first author (WK) thanks JSPS Research Fellowships for their financial support.

## References

- Naselli C, Rabolt JF, Swalen JD (1985) *J Chem Phys* 82:2136 DOI [10.1063/1.448351](https://doi.org/10.1063/1.448351)
- Allara DL, Nuzzo RG (1985) *Langmuir* 1:45 DOI [10.1021/la00061a007](https://doi.org/10.1021/la00061a007)
- Naito KJ (1989) *J Colloid Interface Sci* 131:218 DOI [10.1016/0021-9797\(89\)90161-6](https://doi.org/10.1016/0021-9797(89)90161-6)
- Tsujii Y, Itoh T, Fukuda T, Miyamoto T, Ito S, Yamamoto M (1992) *Langmuir* 8:936 DOI [10.1021/la00039a032](https://doi.org/10.1021/la00039a032)
- Ohmori S, Ito S, Yamamoto M (1990) *Macromolecule* 23:4047 DOI [10.1021/ma00220a004](https://doi.org/10.1021/ma00220a004)
- Oguchi K, Yoden T, Kosaka Y, Watanabe M, Sanui K, Ogata N (1988) *Thin Solid Films* 161:305 DOI [10.1016/0040-6090\(88\)90262-3](https://doi.org/10.1016/0040-6090(88)90262-3)
- Ito T, Tsujii Y, Suzuki H, Fukuda T, Miyamoto T (1992) *Polym J* 24:641 DOI [10.1295/polymj.24.641](https://doi.org/10.1295/polymj.24.641)
- Basque P, Gunzbourg A, Rondeau P, Ritcey AM (1996) *Langmuir* 12:5614 DOI [10.1021/la9507186](https://doi.org/10.1021/la9507186)
- Kasai W, Kuga S, Magoshi J, Kondo T (2005) *Langmuir* 21:2323 DOI [10.1021/la047323j](https://doi.org/10.1021/la047323j)
- Kawaguchi T, Nakahara H, Fukuda K (1985) *Thin Solid Films* 133:29 DOI [10.1016/0040-6090\(85\)90422-5](https://doi.org/10.1016/0040-6090(85)90422-5)
- Xiao Y, Ritcey AM (2000) *Langmuir* 16:4252 DOI [10.1021/la990691g](https://doi.org/10.1021/la990691g)
- Kondo T, Togawa E, Brown RM Jr (2001) *Biomacromolecules* 2:1324 DOI [10.1021/bm0101318](https://doi.org/10.1021/bm0101318)
- Togawa E, Kondo T (1999) *J Polym Sci B Polym Phys* 37:451 DOI [10.1002/\(SICI\)1099-0488\(19990301\)37:5](https://doi.org/10.1002/(SICI)1099-0488(19990301)37:5)
- Kondo T, Nojiri M, Hishikawa Y, Togawa E, Romanovicz D, Brown RM Jr (2002) *Proc Natl Acad Sci U S A* 99:14008 DOI [10.1073/pnas.212238399](https://doi.org/10.1073/pnas.212238399)
- Kondo T, Gray DG (1991) *Carbohydr Res* 220:173 DOI [10.1016/0008-6215\(91\)80015-F](https://doi.org/10.1016/0008-6215(91)80015-F)
- Roberts G (1990) *Langmuir-Blodgett films*. Plenum, New York, p 106
- Rabolt JF, Burns FC, Schlotter NE, Swalen JD (1983) *J Chem Phys* 78:946 DOI [10.1063/1.444799](https://doi.org/10.1063/1.444799)
- Miyashita T, Suwa T (1994) *Langmuir* 10:3387 DOI [10.1021/la00022a005](https://doi.org/10.1021/la00022a005)
- Kojio K, Takahara A, Kajiyama T (2000) *Langmuir* 16:9314 DOI [10.1021/la0004303](https://doi.org/10.1021/la0004303)
- Snyder RG (1960) *J Mol Spectrosc* 4:411 DOI [10.1016/0022-2852\(60\)90103-X](https://doi.org/10.1016/0022-2852(60)90103-X)
- Kaganer VM, Möhwald H, Dutta P (1999) *Rev Modern Phys* 71:779 DOI [10.1103/RevModPhys.71.779](https://doi.org/10.1103/RevModPhys.71.779)
- Lawrie GA, Barnes GT (1994) *J Colloid Interface Sci* 162:36 DOI [10.1006/jcis.1994.1005](https://doi.org/10.1006/jcis.1994.1005)
- Zawisza I, Burgess I, Szymanski G, Lipkowski J, Majewski J, Satija S (2004) *Electrochimica Acta* 49:3651 DOI [10.1016/j.electacta.2004.02.051](https://doi.org/10.1016/j.electacta.2004.02.051)
- Kaganer VM, Brezesinski G, Möhwald H, Howes PB, Kjaer K (1998) *Phys Rev Lett* 81:5864 DOI [10.1103/PhysRevLett.81.5864](https://doi.org/10.1103/PhysRevLett.81.5864)
- Brezesinski G, Kaganer VM, Möhwald H, Howes PB (1998) *J Chem Phys* 109:2006 DOI [10.1063/1.476777](https://doi.org/10.1063/1.476777)